International Journal of Innovative Technology and Exploring Engineering (IJITEE)
ISSN: 2278-3075 (Online), Volume-10 Issue-4, February 2021

Modelling and CFD Simulation of Temperature and Airflow Distribution Inside a Forced Convection Mixed-Mode Solar Grain Dryer with a Preheater

Johannes P. Angula, Freddie Inambao

Abstract: ***In this study, a 3D Computational Fluid Dynamics (CFD) model was developed to simulate the drying process of maize ears/cobs in a mixed-mode solar grain dryer. The dryer system is aimed to operate under forced convection and is integrated with a preheater to heat air prior to entering the solar collector. The 3D model was developed with great accuracy using SolidWorks software and the CFD simulation was carried out using ANSYS Fluent software. The study was aimed at analyzing and predicting temperature and airflow distribution in the mixed-mode solar dryer system. The CFD simulation was conducted at different airflow velocities varying from 0.5 m/s to 2 m/s for different temperature values of the preheater. Results from the simulation of the solar collector were satisfactory, indicating a minimum and maximum temperature of 59.7 °C and 70.5 °C at minimum and maximum drying conditions, respectively. The variation of temperature inside the drying chamber was predicted with an average maximum of 64.1 °C at the inlets. Results of airflow distribution in the solar collector and drying chamber indicated high turbulence and flow recirculation. This is a desirable flow combination that promotes good moisture evaporation from the maize ears during the drying process. This study proves that the use of computer software can allow one to clearly gain an understanding of the development, heat and mass transfer process, and performance of dryers used in the food drying industry. This approach can promote improvements in existing drying processes and increase food productivity.***

Keywords**:** ***Modelling & CFD simulation, Maize ears, Solar drying, Temperature distribution, Air flow distribution***

I. INTRODUCTION

Advances in drying technologies over time have significantly improved food productivity and quality. Amongst the various drying technologies used, solar drying is one of the most efficient and cost-effective for drying food and agricultural products [1]. This technology uses solar radiation from the sun to generate thermal energy which is used in the drying process. The use of solar energy has gained popularity in food drying applications due to the ongoing reduction in natural resources, high natural fuel costs, and environmental damage [2], [3]. To develop an efficient solar dryer one needs to take into consideration the weather conditions and drying parameters which significantly affect the solar dryer's performance. Recent studies on food drying applications rely on the use of Computer-Aided Design (CAD) and Computational Fluid Dynamics (CFD) codes to model and simulate the drying phenomena. The use of CFD codes has gained popularity in the design industry as it is regarded as a promising tool for modeling and simulating designs, making costly experimental trials unnecessary [4]–[6]. CFD is a powerful and innovative computational method that uses numerical calculations and algorithms to solve and analyze problems associated with fluid flow in specified regions of interest [7], [8]. With sufficient simulation results, one gains an understanding of the performance of a dryer at various drying conditions. This allows the actual solar dryer to developed, tested and optimized. This study involves the use of CAD and CFD codes to model and simulate the drying of maize ears/cobs using a forced convection mixed-mode solar grain dryer integrated with a preheater. The CFD code used in this study to simulate the solar dryer system is ANSYS Fluent, while the CAD code used in the design or model creation is SolidWorks. The aim was to develop a three-dimensional model of a mixed-mode solar dryer system and simulate it against various drying parameters to predict the temperature and airflow distribution within the dryer system

II. THEORY

The approach to CFD analysis of the solar dryer involves the computation of the governing equations for the model. Using the CFD code, the kinetics of the fluid are analyzed and solved primarily using the compressible Navier-Stokes partial differential equations given by equation 1 [9] and equation 2 [10]. Equation (1) is referred to as a continuity equation while (2) is referred to as momentum law conservation. In solar drying, heat transfer occurs; hence, an additional equation to incorporate the energy transfer is included in the computation. The heat transfer process is governed by the first thermodynamic law, as expressed by (3) [11].

$$\nabla . \rho \vec{V} + \frac{\partial \rho}{\partial t} = 0 \qquad (1)$$

Manuscript received on November 26, 2020.
Revised Manuscript received on January 25, 2021.
Manuscript published on February 28, 2021.
* Correspondence Author
Johannes P. Angula*, Department of Mechanical Engineering, University of KwaZulu-Natal, Durban, South Africa. Email: 210546069@stu.ukzn.ac.za
Freddie Inambao, Department of Mechanical Engineering, University of KwaZulu-Natal, Durban, South Africa. Email: Inambaof@ukzn.ac.za

$$\underbrace{\rho\left(\frac{\partial \vec{V}}{\partial t}+\vec{V}.\nabla\vec{V}\right)}_{1}-\underbrace{\nabla p}_{2}+\underbrace{\nabla.\left[\mu(\nabla\vec{V}+(\nabla.\vec{V})^{T})-\frac{2}{3}\mu(\nabla.\vec{V})I\right]}_{3}+\underbrace{F}_{4} \quad (2)$$

$$\frac{\partial}{\partial t}(\rho C_a T)+\frac{\partial}{\partial x_j}(\rho u_j C_a T)-\frac{\partial}{\partial x_j}\left(\gamma\frac{\partial T}{\partial x_j}\right)=S_T \quad (3)$$

The preceding equations are essentially a simplification of the sets of equations in rectangular coordinates. In equation 2, term 1 is a representation of the inertial forces acting on the fluid; term 2 represents the effect of thermodynamic forces on the fluid particles, term 3 indicates the impact of the dynamic viscosity of the fluid, while term 4 represents all other external forces acting on the fluid. The drying of maize ears (cobbs) was modelled using the evaporation-condensation model found in the ANSYS Fluent program. It is available with the mixture and Eulerian multiphase models. The transfer of mass during moisture evaporation phases is described by (4) and (5). If the temperature T is greater than the saturation temperature T_{sat}, evaporation will occur in the drying chamber. Hence the transfer of mass during evaporation:

$$m^{\cdot}_{e\to v}=coeff*\alpha_l\rho_l\frac{(T-T_{sat})}{T_{sat}} \quad (4)$$

If the temperature T is less than the saturation temperature T_{sat}, condensation will occur in the drying chamber. Hence the transfer of mass during condensation:

$$m^{\cdot}_{e\to v}=coeff*\alpha_v\rho_v\frac{(T-T_{sat})}{T_{sat}} \quad (5)$$

The process of drying is generally associated with turbulent flows which makes it almost impossible to computationally solve turbulent flows using direct Navier-Stokes partial differential equations. Hence, Navier-Stokes partial differential equations coupled with other transport equations are considered to accurately model turbulence in the fluid domain. Other turbulence models that can be used are the Reynolds Averaged Navier-Stokes (RANS) model and the Large Eddy Simulation (LES) model. More information about the RANS and LES models can be found in literature such as [11]–[14].

III. METHODOLOGICAL APPROACH

The approach to this research work included the use of CAD and CFD codes to develop and simulate the model as required for different drying parameters. The CAD software used to create the model of the solar dryer system was SolidWorks 2018, and the CFD code used for simulating the developed model was ANSYS Fluent 19.2. The simulation results can be validated against the experimental results which helps necessary improvements to be made.

A. Model Creation and Meshing

In this study of analyzing a solar dryer in forced convection and mixed-mode operation integrated with a preheater, a decision was made to divide the entire solar dryer system into three models. This was necessitated due to the model's complexity and, most importantly, to reduce computational time and cost. Fig. 1 shows the models of the solar dryer system which were created using SolidWorks software.

As can be seen in Fig.1, the three models are the solar collector model, the interconnector flow channel model, and the drying chamber model. Each model was imported into ANSYS Fluent and analyzed separately. The output results from the first model were used as input results on the proceeding model. To accurately simulate a CFD problem, the model needed to be correctly meshed. The three meshed models of the solar dryer system are shown in Fig. 2. Essentially, what was meshed is the fluid volume created from the solid body in SolidWorks using the Boolean operation method and imported into ANSYS Fluent. A closer view of the mesh within close proximity of the maize ears contact surfaces is shown in Fig. 3. In this region, the mesh is refined to smaller mesh elements to improve the modeling process's accuracy. The mesh criteria applied to the three models are specified in Table 1. Necessary adjustments were also made to the mesh in refining certain areas of the model, such as using inflation layers, refined mesh size, elements order, etc.

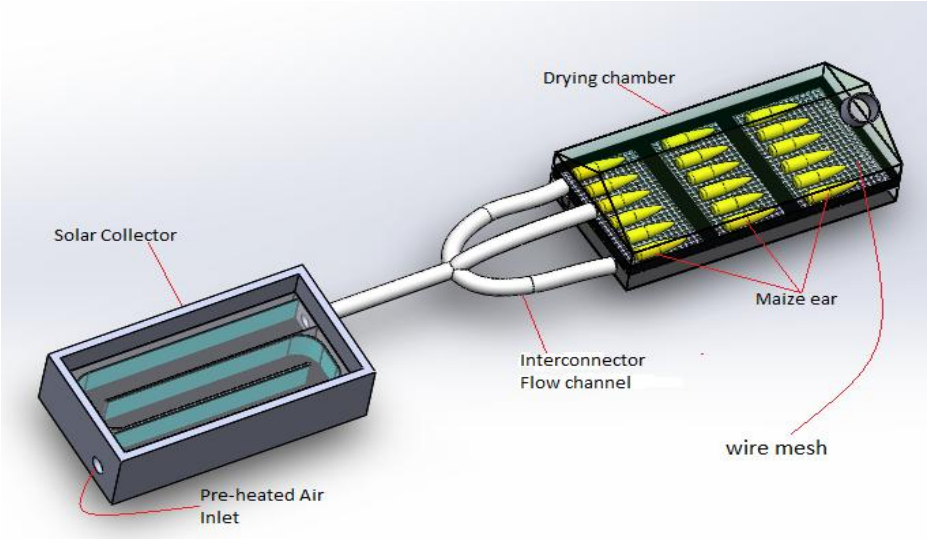

Fig. 1. CFD model of the mixed-mode solar dryer system

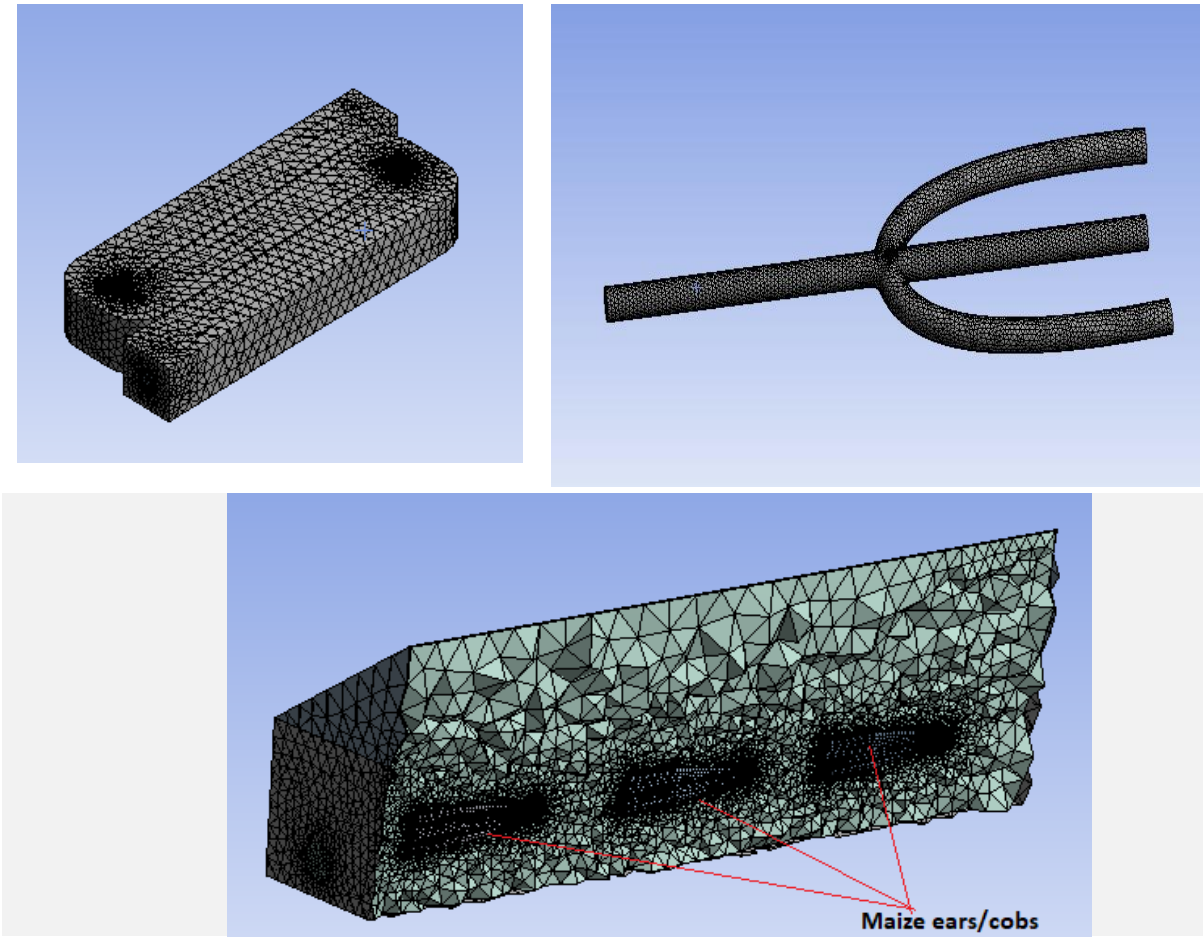

Fig 2. 3D Mesh of the solar collector fluid volume (top left), interconnector flow channel fluid volume (top right), and a cross-sectional view of the drying chamber (bottom center)

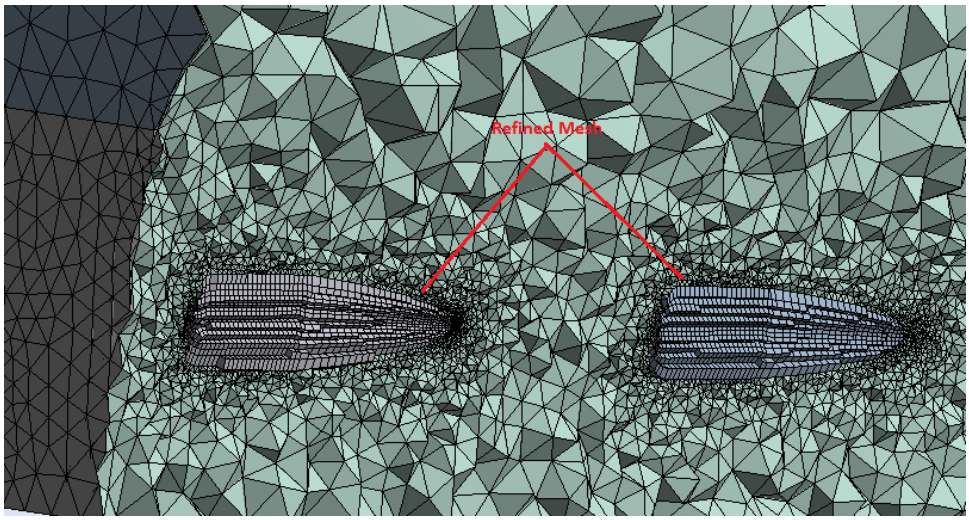

Fig. 3. Closer view of the refined mesh in the drying chamber

Table 1. Mesh criteria applied to the CFD model of the solar dryer system

Applied mesh criteria	CFD Model
Body mesh element size: 8 mm	Solar collector, Interconnector flow channel, Drying chamber
Element size at contact regions: 3 mm	Solar collector, Interconnector flow channel
Element size at contact regions: 2 mm	Drying chamber
Element size at curvature: 0.3 mm	Solar collector, Interconnector flow channel
Element size at curvature: 0.6 mm	Drying chamber

Mesh type: Tetrahedron	Solar collector, Interconnector flow channel, Drying chamber
Number of inflation layers: 5 layers	Solar collector, Interconnector flow channel
Number of inflation layers: 7 layers	Drying chamber
Elements order: Quadratic	Drying chamber
Mesh quality: Medium	Drying chamber

B. Definition of the Model

The simulation of the model conducted in this study was carried out based on several assumptions that were put in place to simplify the model. This was necessary as some of the flow characteristics are complex and impractical to achieve with the available computational resources and power. The main assumptions that were considered were:

- Steady state conditions are assumed for constant solar irradiation.
- The initial moisture content of grains inside the drying chamber is the same.
- The initial temperature of grains is the same as the drying air temperature inside the drying chamber.
- All incident solar irradiation falling on the solar dryer system are Direct Normal Irradiation (DNI) rays, equivalent to the measured average DNI rays of the site location.
- Negligible heat loss around the solar dryer system.
- Incident solar irradiation absorbed by the glazing material of the solar dryer system is neglected.

The above assumptions facilitated the definition of the three meshed models of the solar dryer system, enabling various boundary conditions to be assigned as required for simulation purposes. The simulation was conducted before the experiment. Hence, the weather parameters were assumed based on the calculated average data collected over the past 3 years from the Virginia Weather Station in Durban. Due to Durban's weather conditions that rarely exceed 30 °C, the presence of the preheater allows the ambient air temperature to be varied before entering the solar collector. It was considered that the drying air be preheated between 30 °C and 40 C°. For the purpose of the simulation, the preheater's effect was modelled as direct input values of temperature and calculated values of relative humidity. This was because the preheater used during the experiment has a temperature controller. The simulation was conducted using the pre-set output temperature and relative humidity values from the preheater, which served as the solar collector's input air flow values. The output temperature and relative humidity at the preheater outlet were 30 °C & 39%, 36 °C & 28%, and 40°C & 23%, respectively. Table 2 shows the boundary conditions that were applied to each model component of the solar dryer system.

Table 2. Applied boundary conditions of the solar dryer system at different drying airflow velocities and preheater temperatures

Boundary conditions	Model component 1: Solar collector	Model component 2: Interconnector flow channel	Model component 3: Drying chamber
Inlet flow conditions	Temperature: 30 °C Relative humidity: 39 % Flow velocity: 0.5 m/s Turbulence intensity: 8 %	Temperature: using output values from solar collector. Relative humidity: using output values from solar collector. Flow velocity: using output values from solar collector.	Temperature: using output values from interconnector flow channel. Relative humidity: using output values from interconnector flow channel. Flow velocity: using output values from interconnector flow channel. Turbulence intensity: 5 %
Outlet flow conditions	Pressure outlet Pressure value: 1 atm	Same conditions as solar collector	Same conditions as solar collector
Multiphase Model	-	-	Eulerian model with evaporation-condensation as the Eulerian parameter under Lee model. Eulerian phases number: 3 Volume fraction parameter: Implicit formulation Evaporation frequency: tuned to 50 Saturation temperature: default set
Viscous Model setup	Viscous model: Realizable $k-\varepsilon$ model with standard wall functions	Same conditions as Solar collector	Viscous model: Realizable $k-\varepsilon$ model with enhanced wall treatment
Energy setup	Energy model: active surface-to-surface radiation mode used. Heat flux on absorber surface: 155.8 W/m^2	No heat transfer, it has an adiabatic wall	Same conditions as solar collector

Materials	Solid material: Copper Solid material density: 8 978 kg/m^3 Specific Heat: 381 J/kg.K Thermal conductivity: 387.6 W/m.k Fluid: Air Fluid properties: ANSYS Fluent default values	Fluid is sir using default properties	*Aluminium for the drying tray* Density: 2 700 kg/m^3 Specific Heat: 880 J/kg.K Thermal conductivity: 189 W/m.K *Perspex glass* Density: 1190 kg/m^3 Specific Heat: 1270 J/kg.K Thermal conductivity: 0.189 W/m.K *Maize ear* Density: 760 kg/m^3 Specific Heat [6]: = $1.3066 + 1.2045M_d + 0.0198T$ Thermal conductivity [6]: $= 0.028 + 0.1321M_d + 3.4981 \times 10^{-3}T - 0.128M_d^2 - 2.24 \times 10^{-5}T^2$
Solver	Pressure based	Pressure based	Pressure based
Solution methods	Coupling: Pressure to velocity using SIMPLEC Skewness correction factor of 1 with least square cell-based method. Hybrid initialization	Same conditions as solar collector	Same conditions as solar collector
Calculation setup	Maximum iterations: 100 to 200 Residual errors: 0.0001	Same conditions as solar collector	Same conditions as solar collector

In Table 2 "T" and "M_d" are the maize ear's temperature and moisture content, respectively. The simulation was repeated for all the previously mentioned preheater output conditions at an airflow velocity of 1 m/s and 2 m/s

IV. RESULTS AND DISCUSSION

The results obtained from CFD simulations are shown in Fig. 7, Fig. 8, Fig. 9, and Fig. 10. Due to the complexity of the model and simulation parameters, the maize cobs' final moisture content could not be determined through simulation. However, the temperature and velocity profile across different solar dryer system components during the predicted drying process are presented. In addition, the corresponding airflow distribution across the solar collector and drying chamber are also presented. To have a glimpse of the dryer performance as simulated at different drying parameters, the results shown in the figures are only for minimum and maximum drying parameters. Fig. 7 and Fig. 8 show the results of temperature distribution and velocity profile across the solar collector at minimum and maximum drying conditions. In this study, conditions at minimum drying were considered to be when the solar dryer system was operating as a natural convection solar dryer without a preheater. This is presented with an airflow velocity of 0.5 m/s and preheater temperature of 30 ℃ in the simulation process. While conditions at maximum drying are presented with the maximum airflow velocity of 2 m/s and 40 ℃ preheater temperature that were considered for simulation purposes.

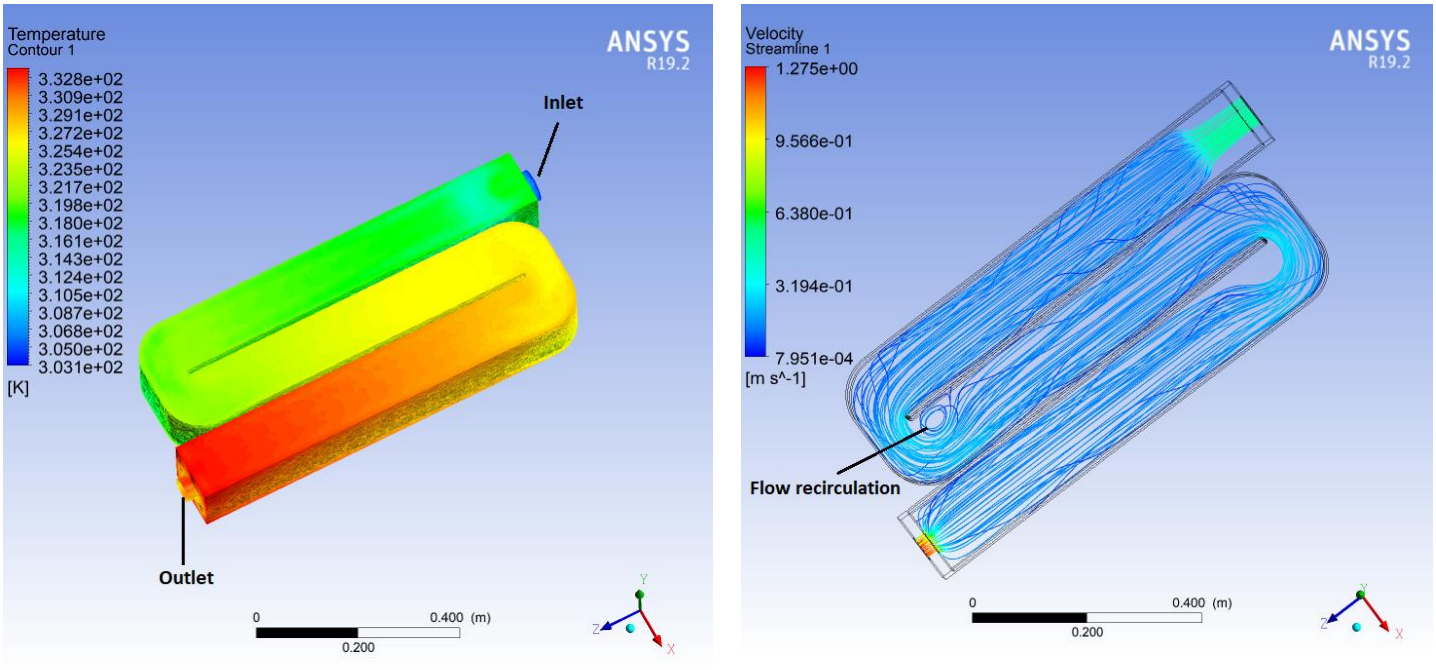

Fig. Temperature distribution (left) at 30 ℃ preheated air and velocity profile (right) at 0.5 m/s airflow across the solar collector

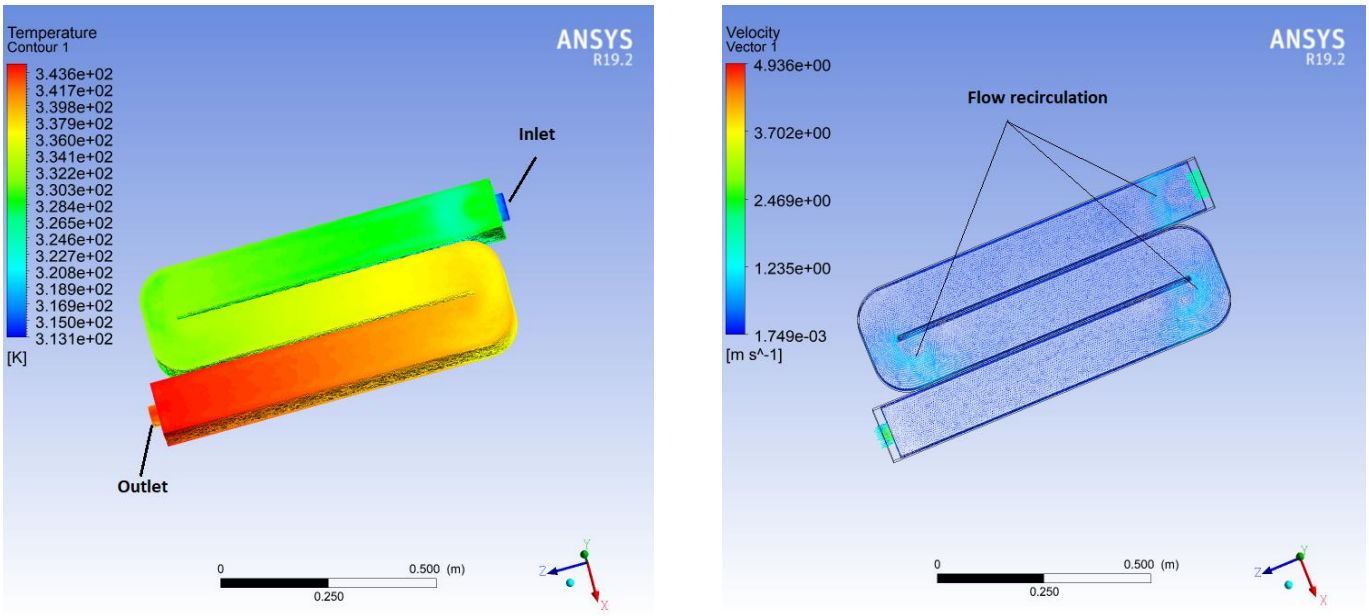

Fig. 8. Temperature distribution (left) at 40 ℃ preheated air and velocity profile (right) at 2 m/s airflow across the solar collector

The temperature distributions shown in Fig. 7 and Fig. 8 are very similar, however the temperature readings across the solar collector differ at various points along the air flow channel. It is evident that air starts heating up from the inlet as it navigates through the flow channel and gains its highest temperature toward the solar collector outlet. As shown in Fig. 7, at 30 ℃ preheated air, a maximum temperature of 332.8 K (59.7 ℃) is predicted at the outlet when the airflow is set to 0.5 m/s, while at 40 ℃ preheated air, a maximum temperature of 343.6 K (70.5 ℃) is predicted at the outlet when the airflow is set to 2 m/s. The presence of flow recirculation and turbulence inside the solar collector is also predicted, as shown by the velocity profile.

The flow exiting the solar collector is transferred to the drying chamber through an insulated interconnector flow channel. There were no results of the temperature profile across the interconnector flow channel since it is assumed that it is completely insulated, and there is no heat transfer across it. Thus, the airflow entering the interconnector will exit at the same temperature as it enters. However, its flow velocity will differ at the exit because of the change in areas. Using the solar collector and interconnector flow channel results, the temperature distribution and flow velocity profile across the drying chamber were obtained as shown in Fig. 9 and Fig. 10, respectively.

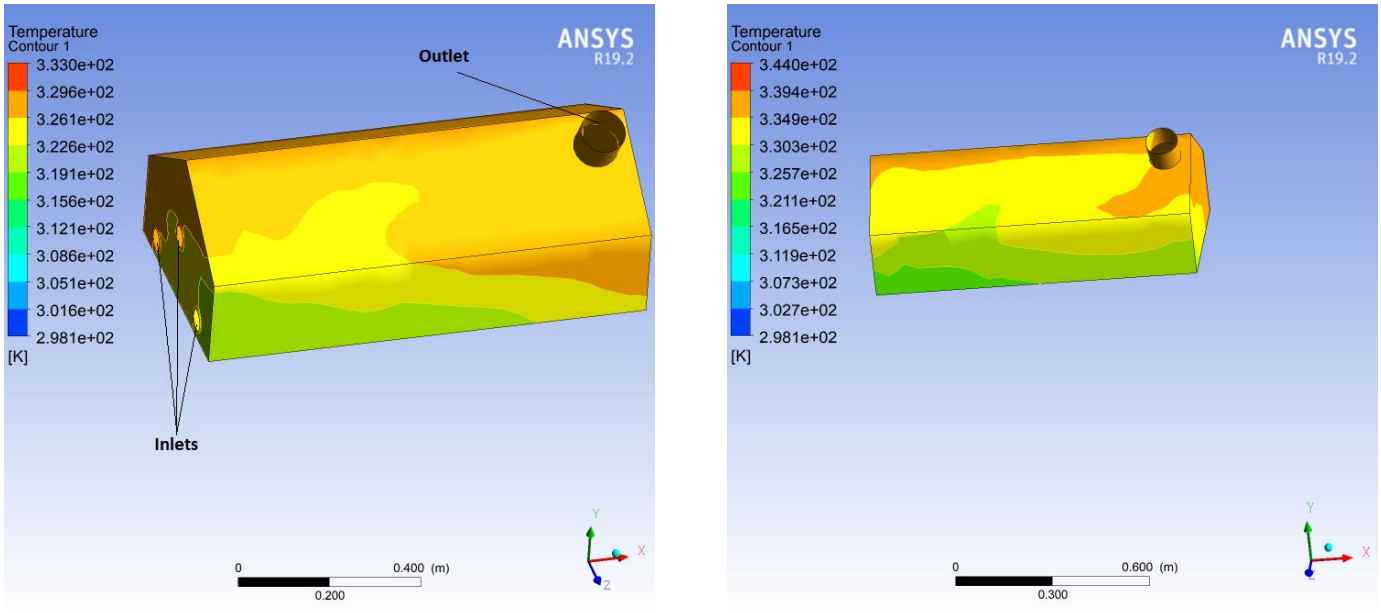

Fig. 9. Temperature distribution at 30 ℃ preheated air (left) and temperature distribution at 40 ℃ preheated (right) across the drying chamber during drying process

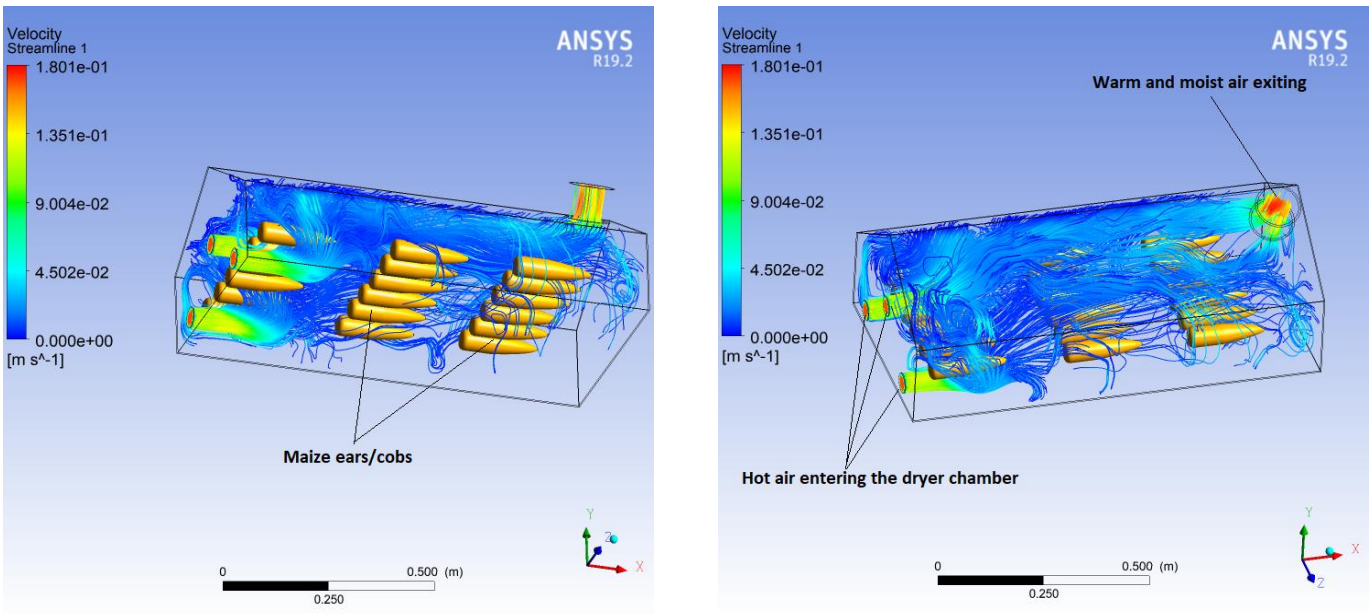

Fig. 10. Airflow distribution inside the drying chamber during drying process

The simulation results indicate the temperature profile across the drying chamber predicts temperature varying across the drying chamber. During the drying process, different chamber regions will have experienced different temperatures due to the heat and mass transfer processes. The results were also affected by the position of the sun at the time of drying. The highest temperatures as shown in Fig. 9 occur near the inlets when hot air enters the drying chamber. The average minimum temperature in the drying chamber was predicted to be around 327.9 K (54.8 ℃), while the average maximum temperature was about 337.2 K (64.1 ℃).

The flow behavior inside the drying chamber as shown in Fig. 10 during the drying process, predicts severe flow turbulence and recirculation. This is necessary during the drying process to accelerate the evaporation of moisture from the grains. The profile also indicates that more air flow is expected in the upper portion of the drying chamber than the bottom. Due to moisture evaporation, warm and moist air will exit the drying chamber at a relatively low velocity and at a temperature which is higher than ambient temperature.

V. CONCLUSION

In this study, a forced convection mixed-mode solar grain dryer with a preheater was modelled using SolidWorks and CFD simulation was carried out using ANSYS Fluent. Due to the complexity of the model and available computational resources, several assumptions were taken into consideration during the simulation process to simplify the problem. The solar dryer system was modelled and simulated with great accuracy. The simulation was run at a flow velocity varying from 0.5 m/s to 2 m/s for different temperature values of the preheater.

The results of temperature distribution indicated a maximum temperature of 70.5 ℃ predicted at the solar collector outlet for maximum drying conditions, and a maximum temperature of 59.7 ℃ at the solar collector outlet for minimum drying conditions. Due to the effect of mixed-mode solar drying, the average maximum temperature in the drying chamber was predicted to be around 64.1 ℃. A small percentage of condensation is also expected to occur within some areas of the drying chamber. The simulation predicted a satisfactory airflow distribution within the drying chamber, indicating heavy flow turbulence and recirculation around the maize ears/cobs. The provision of multiple flow inlets at the drying chamber enable a perfect flow distribution and enhances moisture evaporation from the maize ears. Based on the results obtained, it is evident that increasing both the drying air velocity and temperature at the inlet of the solar collector improves the drying process of solar grain dryers.

REFERENCES

1. O. V. Ekechukwu, and B. Norton, "Design and measured performance of a solar chimney for natural-circulation solar-energy dryers," *Renewable Energy*, vol. 10 no. 1, 1997, pp. 81-90. https://doi.org/10.1016/0960-1481(96)00005-5.
2. P. Demissie, M. Hayelom, A. Kassaye, A. Hailesilassie, M. Gebrehiwot and M. Vanierschot, "Design, development and CFD modeling of indirect solar food dryer," Proceedings of the 10th International Conference on Applied Energy, Hong Kong. Energy Procedia, vol. 158, 2019, pp. 1128-1134. https://doi.org/10.1016/j.egypro.2019.01.278.
3. A. Lingayat, V. P. Chandramohan and V. R. K. Raju, "Design, development and performance of indirect type solar dryer for banana drying," *Energy Procedia*, vol. 109, 2017, pp. 409-416. https://doi.org/10.1016/j.egypro.2017.03.041.
4. P. D. Tegenaw, M. G. Gebrehiwot and M. Vanierschot, "Design and CFD modeling of a solar food drier," Proceedings of the 6th European Drying Conference, Belgium. Euro Drying, June 2017, pp. 183–184.
5. Y. Amanlou and A. Zomorodian, "Applying CFD for designing a new fruit cabinet dryer," *Journal of Food Engineering*, vol. 101, no. 1, 2010, pp. 8-15, https://doi.org/10.1016/j.jfoodeng.2010.06.001.
6. T Norton, B. Tiwari and D. W. Sun, "Computational fluid dynamics in the design and analysis of thermal processes: a review of recent advances," *Critical Review in Food Science and Nutrition*, vol. 53, no. 3, pp. 2013, 251-275. https://doi.org/10.1080/10408398.2010.518256.
7. A. A. Ambesange and S. K. Kusekar, "Analysis of flow through solar dryer DUCT using CFD," *International Journal of Engineering Development and Research*, vol. 5, no. 1, 2017.
8. T. Norton and D. W. Sun, "CFD: An innovative and effective design tool for the food industry." In *Food Engineering Interfaces*, J. Aguilera, R. Simpson, J. Welti-Chanes, D. Bermudez-Aguirre, ands G. Barbosa-Canovas, (Eds). Food Engineering Series. New York, NY: Springer, 2010, pp. 55-68. https://doi.org/10.1007/978-1-4419-7475-4_3.
9. W. R. Fox, J. P. Pritchard and T. A. Macdonald. Introduction to Fluid Mechanics. 7th ed. New Delhi, India: John Wiley & Sons, 2010, pp. 161-205.
10. COMSOL INC. Navier-Stokes Equations. In *Multiphysics Cyclopedia*, 2017. Available at https://www.comsol.com/multiphysics/navier-stokes-equations.
11. J. T. Norton and D. W. Sun, "Computational fluid dynamics (CFD) – an effective and efficient design and analysis tool for the food industry: a review," *Trends in Food Science & Technology*, vol. 17, no. 11, 2006, pp. 600-620. https://doi.org/10.1016/j.tifs.2006.05.004.
12. J. Guerrero. *Introduction to Computational Fluid Dynamics: Governing Equations, Turbulence Modelling Introduction and Finite Volume Discretization Basics*. 2015. https://doi.org/10.13140/RG.2.1.1396.4644.
13. I. Sadrehaghighi. *Turbulence Modeling – A Review. CFD Open Series, Patch* 1.85.9, 2019. https://doi.org/10.13140/RG.2.2.35857.33129/2.
14. S. Pope. *Turbulent Flows*. Cambridge: Cambridge University Press, 2000.

AUTHOR PROFILES

Johannes P. Angula holds a BSc Mechanical Engineering from the University of KwaZulu-Natal, South Africa. He has worked as a locomotive maintenance engineer and, research and development engineer for 5 years. His area of research focuses on renewable and green energy technologies with emphasis on solar drying systems. Mr. Angula is a member of the Engineering Council of Namibia and has published three articles on solar drying, computational fluid dynamics (CFD) in solar drying, and on the optimization of solar dryers through thermal energy storage systems.

Professor Freddie Inambao holds an MSc and Ph.D. (Technical Sciences) from Volgograd Polytechnic Institute, Russia. He has lectured in several Universities: University of Zambia, University of Botswana, University of Durban-Westville and University of KwaZulu-Natal (UKZN). Professor Inambao is a Principal Advisor of the Green Energy Solutions Research Group (UKZN). Professor Inambao's research and educational efforts focus on: energy efficiency, alternative energy systems, renewable energy, energy management, energy audit, energy and fuels, HVAC, low temperature power generation; water purification and desalination. Professor Inambao has directly supervised and graduated more than 30 MSc, Ph.D students and postdoctoral associates and is currently supervising over 20 postgraduates: He is author of more than 130 articles in peer-reviewed international journals and 130 conference proceedings, a co-author of 12 books and two chapters in books. Professor Inambao is a recipient of several prestigious awards: Top 30 Publishing Researcher Award for 2016 to 2019 UKZN; College of Agriculture, Engineering and Science Research Awards 2019; JW Nelson Research Productivity Award for 2013 to 2019.

NOMENCLATURE

∇	Vector operator
$\vec{V}$	Fluid velocity (m/s)
t	Time (m)
ρ	flow density (kg/m^3)
μ	fluid dynamic viscosity (kg/m.s)
p	local thermodynamic pressure (N/m^2)
C_a	specific heat capacity of the fluid (W/kg.K)
T	temperature of the fluid (K)
x_i	rectangular coordinate (m) of the fluid element
u_i	fluid velocity component in the respective coordinate
γ	thermal conductivity (W/m.K)
S_T	Energy added or work done on the fluid element (J)
$coeff$	Coefficient that must be fine-tuned and can be interpreted as a relaxation time
α_l	Liquid volume fraction
ρ_l	Liquid density (kg/m^3)
α_v	Vapor volume fraction
ρ_v	Vapor density (kg/m^3)
$\dot{m_{e\to v}}$	Transfer of mass during evaporation or condensation